AMERICAN COLLEGE
of RHEUMATOLOGY
Empowering Rheumatology Professionals

Citrullinated Inhibitor of DNA Binding 1 Is a Novel Autoantigen in Rheumatoid Arthritis

Ray A. Ohara,[1] Gautam Edhayan,[1] Stephanie M. Rasmussen,[1] Takeo Isozaki,[2] Henriette A. Remmer,[1] Thomas M. Lanigan,[1] Phillip L. Campbell,[1] Andrew G. Urquhart,[3] Jeffrey N. Lawton,[3] Kevin C. Chung,[3] (ID) David A. Fox,[1] and Jeffrey H. Ruth[1]

Objective. To explore the intrinsic role of inhibitor of DNA binding 1 (ID-1) in rheumatoid arthritis (RA) fibroblast-like synoviocytes (FLS) and to investigate whether ID-1 is citrullinated and autoantigenic in RA.

Methods. RA patient serum ID-1 levels were measured before and after infliximab treatment. RA FLS were transfected with a clustered regularly interspaced short palindromic repeat (CRISPR)/CRISPR-associated protein 9 construct targeting ID-1 to examine the effects of ID-1 deletion. RA synovial fluid (SF) and homogenized synovial tissue (ST) were immunoprecipitated for ID-1 and measured for citrullinated residues using an enzyme-linked immunosorbent assay and Western blotting. Liquid chromatography tandem mass spectrometry (LC-MS/MS) was performed on in vitro–citrullinated recombinant human ID-1 (cit–ID-1) to localize the sites of citrullination. Normal and RA sera and SF were analyzed by immunodot blotting for anti–citrullinated protein antibodies (ACPAs) to cit–ID-1.

Results. RA patient serum ID-1 levels positively correlated with several disease parameters and were reduced after infliximab treatment. RA FLS displayed reduced growth and a robust increase in interleukin-6 (IL-6) and IL-8 production upon deletion of ID-1. ID-1 immunodepletion significantly reduced the levels of citrullinated residues in RA SF, and citrullinated ID-1 was detected in homogenized RA ST (n = 5 samples; $P < 0.05$). Immunodot blot analyses revealed ACPAs to cit–ID-1 but not to native ID-1, in RA peripheral blood (PB) sera (n = 30 samples; $P < 0.001$) and SF (n = 18 samples; $P < 0.05$) but not in normal PB sera. Following analyses of LC-MS/MS results for citrullination sites and corresponding reactivity in immunodot assays, we determined the critical arginines in ID-1 for autoantigenicity: R33, R52, and R121.

Conclusion. Novel roles of ID-1 in RA include regulation of FLS proliferation and cytokine secretion as well as autoantigenicity following citrullination.

INTRODUCTION

Inhibitor of DNA binding 1 (ID-1) is a nuclear transcription factor containing a helix-loop-helix domain that it utilizes to regulate cell growth and differentiation via selective binding and sequestering of distinct transcription factors. By this method, ID-1 controls transcriptional activation of target genes. ID-1 is also known to be actively transcribed in cells exhibiting hyperproliferative responses and is regarded as a marker of cellular self-renewal. Rheumatoid arthritis (RA) synovial fluid (SF) contains abundant amounts of ID-1, and the primary source is activated RA fibroblast-like synoviocytes (FLS). Once released, ID-1 acts as a potent inducer of angiogenesis and also exhibits endothelial progenitor cell chemotactic activity (1), suggesting that ID-1 may contribute to angiogenesis and vasculogenesis by independent mechanisms. ID-1 is packaged into exosomes, which are released from FLS and potentially delivered to other inflammatory cells within RA synovium (2). Although the concept of a secreted nuclear protein may be unconventional, a similar phenomenon occurs in the inflamed joint with DEK, a nuclear protein that functions as a regulator of transcription involved in chromatin architecture

and messenger RNA processing. DEK is secreted by macrophages, found in exosomes, can be detected in the SF of juvenile arthritis patients, and is both an autoantigen and a potent neutrophil chemotactic factor (3,4).

In the current study, we investigated 3 potential key roles for ID-1 in RA: first, as a secreted nuclear protein whose levels correlate with several disease parameters; second, as a regulator of cell proliferation and inflammatory cytokine production by FLS; and third, as a citrullinated autoantigen. We assessed the roles of ID-1 in FLS by use of clustered regularly interspaced short palindromic repeat (CRISPR)/CRISPR-associated protein 9 (Cas9) targeting of ID-1. Immunoassays were used to measure citrullinated ID-1 (cit–ID-1) in synovial tissue (ST). Mass spectrometry was used to define the specific arginines within ID-1 that are converted to citrulline as well as the identity of specific citrulline residues that render ID-1 autoantigenic. The results suggest multidimensional contributions of ID-1 and cit–ID-1 to the pathogenesis of RA.

PATIENTS AND METHODS

Patient samples. Data were collected from a cohort of 27 RA patients (2009–2012), who met the 1987 American College of Rheumatology (ACR) classification criteria (5) for RA. Twenty-seven serum samples (median patient age 49 years [range 21–76]) were collected from the patients before the initial treatment with infliximab. All RA patients were receiving methotrexate and 14 were receiving additional disease-modifying antirheumatic drugs (sulfasalazine or bucillamine). Fourteen age- and sex-matched healthy volunteers (median age 42.5 years [range 29–55]) were recruited as controls. All specimens were obtained with written informed consent and collected following approval from the Showa University Institutional Review Board (IRB). SF samples were obtained from RA patients during arthrocentesis and stored at –80°C in aliquots after centrifugation to remove SF cells. ST samples were obtained from RA patients undergoing total joint replacement and were snap-frozen (liquid nitrogen) in 10% DMSO in fetal bovine serum and stored at –80°C. These samples were obtained, with IRB approval, from RA patients who met the ACR criteria for RA.

Enzyme-linked immunosorbent assay. Patient samples and normal control samples were analyzed using enzyme-linked immunosorbent assay (ELISA) kits for human ID-1 (MyBioSource) and rheumatoid factor (RF; Alpha Diagnostic International). For the ID-1 targeting experiments, cell culture supernatants were measured with ELISA kits for human interleukin-13 (IL-13), epithelial neutrophil–activating peptide 78 (ENA-78/CXCL5), IL-6, and IL-8 (R&D Systems). (For detection of citrulline residues by ELISA [cit-ELISA], see Supplementary Methods, on the *Arthritis & Rheumatology* web site at http://onlinelibrary.wiley.com/doi/10.1002/art.40886/abstract.)

CRISPR/Cas9 targeting of ID-1. CRISPR U6gRNA-pCMV-Cas9-2A–red fluorescent protein (RFP) plasmid (Sigma-Aldrich) containing the guide RNA (gRNA) 5′-GAATCATGAAAGTCGCCAGTGG-3′ was designed to target the human ID-1 gene. CRISPR human EMX1-s4 positive control plasmid (no. CRISPR11-1EA; Sigma-Aldrich) and CRISPR plasmid targeting an irrelevant gene (e.g., *THBS1*) were used as controls. All transfections were performed by electroporation using Amaxa Nucleofector Technology (Lonza). Transfected cells were sorted for fluorescent marker (RFP or green fluorescent protein [GFP]) via fluorescence-activated cell sorting (FACS) and analyzed for CRISPR/Cas9 activity by Tracking of Indels by Decomposition (TIDE) using Desktop Genetics web tool (6). To verify ID-1 depletion, transfected cells were lysed in radioimmunoprecipitation assay (RIPA) buffer supplemented with EDTA-free protease inhibitor cocktail (ThermoFisher Scientific) and analyzed by Western blotting. For assays of cell proliferation and cytokine expressions, sorted cells were plated in 96-well plates (6,000–10,000 cells/well) in complete cell culture medium and imaged hourly for 120 hours using the IncuCyte S3 Live Cell Analysis System (Essen Biosciences). Cell culture supernatants were collected at 24 hours postseeding for analysis by ELISA.

Immunoprecipitation. For ID-1 pulldown experiments, a Direct Immunoprecipitation kit (ThermoFisher Scientific) was used with polyclonal rabbit anti–ID-1 antibodies (nos. ab170511 and ab192303; Abcam) or with rabbit IgG isotype control (ThermoFisher Scientific). RA ST (~0.5 cm^3) homogenates were prepared in ice-cold RIPA buffer supplemented with EDTA-free protease inhibitor cocktail using an electric homogenizer and were centrifuged and filtered (45 μm) to collect the supernatant. For all immunoprecipitation experiments, manufacturers' kit protocols were followed. Samples were eluted with low-pH elution buffer supplied in the kit and prepared in Laemmli sample buffer for Western blotting; flowthroughs were retained for ELISA. All sera, SF, and ST homogenates were incubated with polyclonal goat anti-human IgM (μ-chain specific)–conjugated Agarose (Sigma-Aldrich) at 4°C overnight for removal of RF prior to all immunoassays.

Citrullination of recombinant human ID-1 protein. Recombinant human ID-1 protein (rhID-1) (OriGene Technologies) was citrullinated in vitro using recombinant human peptidylarginine deiminase 4 (rhPAD4) enzyme (Cayman Chemical) or rabbit PAD enzyme (Sigma-Aldrich) as previously described (7). The preparation of noncitrullinated ID-1 (noncit–ID-1) was performed similarly, with cell culture–grade water (Sigma-Aldrich) in place of PAD enzymes.

Western blotting. Citrullinated and noncitrullinated proteins (100 ng each) and IP-eluted samples from RA ST homogenates (30 μl) were prepared in Laemmli sample buffer and were resolved by sodium dodecyl sulfate–polyacrylamide gel electrophoresis (SDS-PAGE) before transfer to nitrocellulose membranes (NCMs) using a semi-dry transfer cell (Bio-Rad).

Blots were washed with 0.05% Tween 20 in Tris buffered saline (TBST) between all subsequent steps. After blocking in 5% nonfat dry milk in TBST, the blots were probed with monoclonal rabbit anti–ID-1 (1:1,000 dilution) (no. TA310605, clone EPR7098; OriGene Technologies) and then probed with horseradish peroxidase–linked anti-rabbit IgG (1:1,000 dilution) (no. 7074; Cell Signaling Technology). SuperSignal West Dura Extended Duration Substrate (ThermoFisher Scientific) was used for detection prior to image acquisition with an Amersham Imager 600 (GE Healthcare Life Sciences). (For detection of citrulline residues by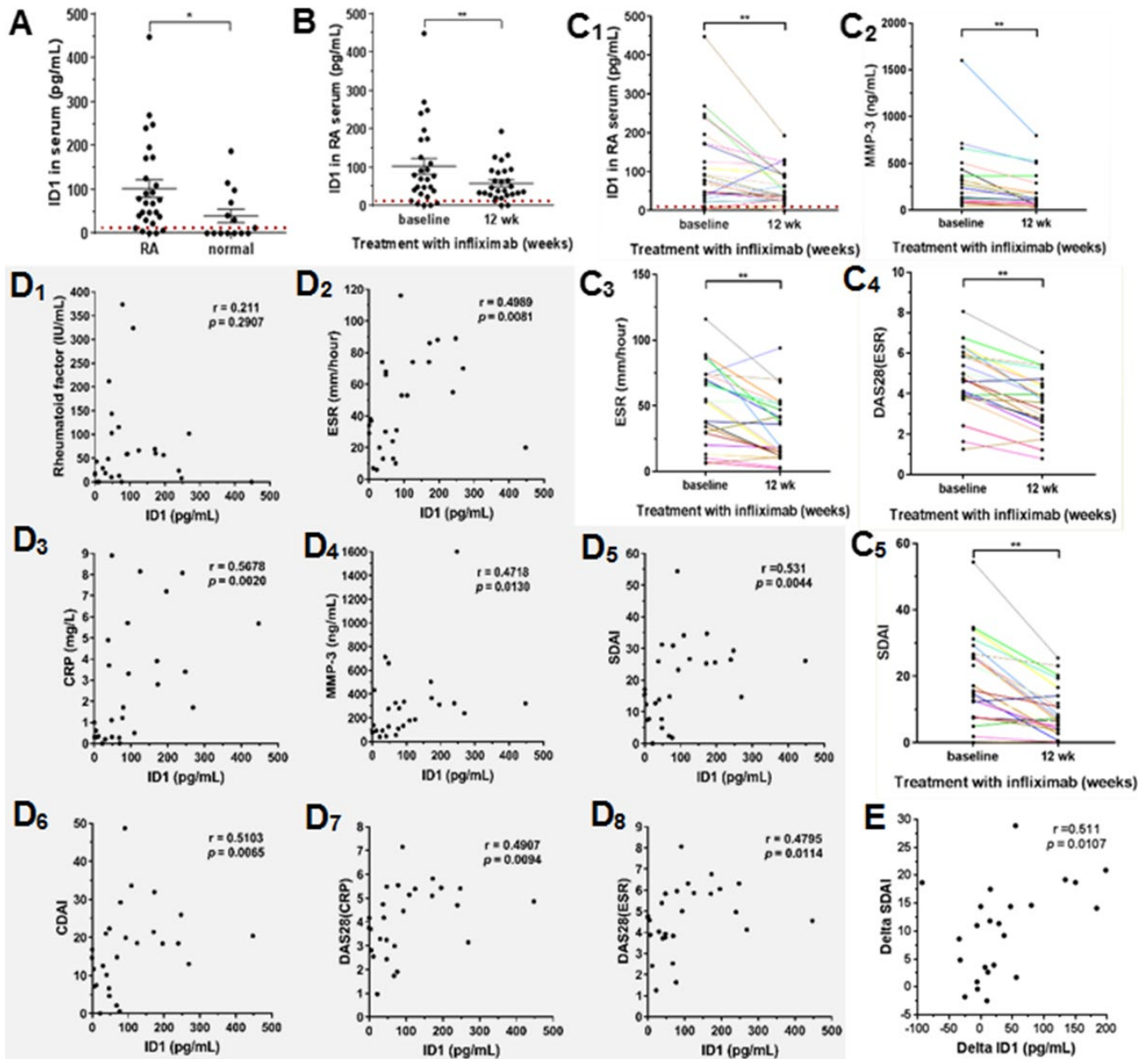 Western blotting, see Supplementary Methods, available at http://onlinelibrary.wiley.com/doi/10.1002/art.40886/abstract.)

Figure 1. Effect of infliximab treatment on serum inhibitor of DNA binding 1 (ID-1) levels in patients with rheumatoid arthritis (RA), and clinical correlations. **A**, ID-1 levels were elevated in RA serum (n = 27) compared to those in serum from age- and sex-matched normal controls (n = 14). **B**, Serum ID-1 levels in patients were decreased at the 12-week time point following infliximab treatment. The red broken line indicates the detection limit of the ID-1 enzyme-linked immunosorbent assay (7.81 pg/ml). Bars in **A** and **B** represent the mean ± SEM. **C**, ID-1 levels and clinical parameters were decreased following treatment with infliximab. Each colored line represents a single patient. **D**, Baseline serum ID-1 levels correlated with various clinical and laboratory parameters. **E**, Change in ID-1 levels from baseline to posttreatment correlated with change in the Simplified Disease Activity Index (SDAI), showing improved SDAI scores with decreased ID-1 levels (n = 24). * = $P < 0.05$; ** = $P < 0.01$. MMP-3 = matrix metalloproteinase 3; ESR = erythrocyte sedimentation rate; DAS28 = Disease Activity Score in 28 joints; CRP = C-reactive protein; CDAI = Clinical Disease Activity Index. Color figure can be viewed in the online issue, which is available at http://onlinelibrary.wiley.com/doi/10.1002/art.40886/abstract.

In-gel digestion and liquid chromatography tandem mass spectrometry (LC-MS/MS). LC-MS/MS was performed by Proteomics and Peptide Synthesis Core at the University of Michigan (Supplementary Methods, http://onlinelibrary.wiley.com/doi/10.1002/art.40886/abstract).

Immunodot blotting. Samples were dotted onto NCMs at 10 ng/dot and blocked in 5% goat serum (Sigma-Aldrich) in TBS. Blots were incubated in either samples (RA SF or PB serum, normal PB serum; 1:10,000 dilution), normal human IgG control (1 μg/ml) (no. 1001A; R&D Systems),

or control antibodies, including monoclonal mouse anti–ID-1 (no. ab66495, clone 2456C1a; Abcam) and polyclonal rabbit anti-PAD4 (1 μg/mL) (no. ab50247; Abcam), then probed with peroxidase AffiniPure goat anti-human IgG (1 μg/ml, dilution 1:5,000) (no. 109035003; ImmunoResearch). To verify specificity for cit–ID-1 reactivity of RA specimens, additional control blots were included on the same NCMs using various proteins including noncit–ID-1, bovine serum albumin (BSA), cit-BSA, ENA-78, cit–ENA-78, and rhPAD4. Densitometry analysis was performed using ImageJ (National Institutes of Health).
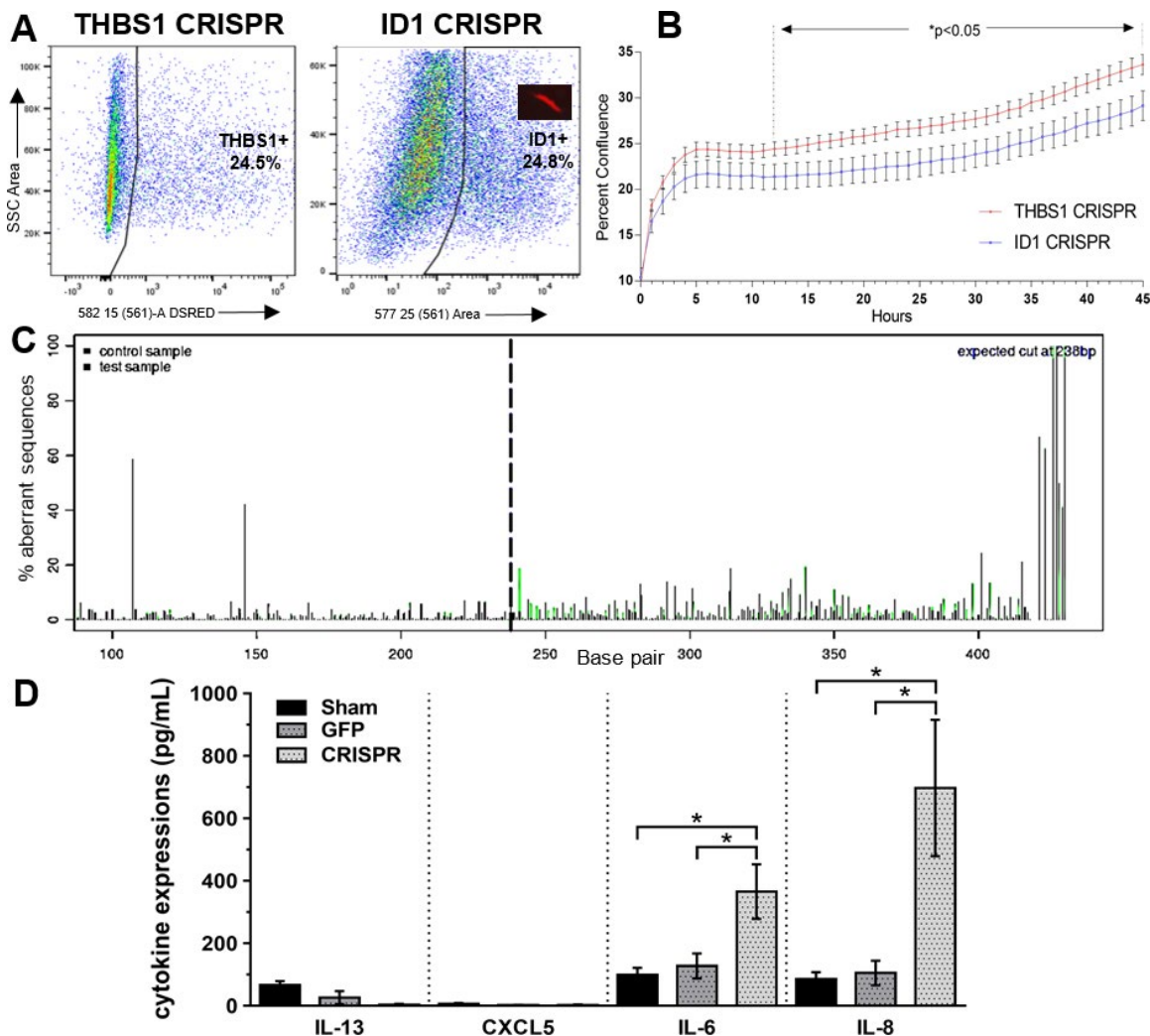

Figure 2. Transfection of RA fibroblast-like synoviocytes (FLS) with clustered regularly interspaced short palindromic repeat (CRISPR)/CRISPR-associated protein 9 (Cas9) plasmid with guide RNA targeting the ID-1 gene. **A,** Fluorescence-activated cell sorting of RA FLS that were transfected with ID-1 CRISPR/Cas9 plasmid or control *THBS1* CRISPR/Cas9 plasmid is shown. **B,** RA FLS transfected with ID-1 CRISPR/Cas9 plasmid (n = 9) or *THBS1* control plasmid (n = 19) were assayed for cell proliferation using the IncuCyte S3 Live-Cell Analysis System. **C,** Due to imperfect repair by Cas9 nuclease, DNA in the cell pool contained a mixture of indels, yielding a composite sequence trace after the break site (black dashed line). An overview of Tracking of Indels by Decomposition algorithm and output is shown, consisting of visualization of aberrant sequence signal in controls (black) and treated samples (green). Cas9 nuclease cut the genome, and the cell repaired the damage caused by nonhomologous end–joining resulting in aberrant sequences. **D,** RA FLS transfected with sham control (n = 17 or more per experiment), green fluorescent protein (GFP) control (n = 5 per experiment), or ID-1 CRISPR/Cas9 plasmid (n = 5 or more per experiment) were sorted and cultured for 24 hours for cytokine expression analysis using enzyme-linked immunosorbent assays. Values are the mean ± SEM. * = *P* < 0.05. IL-13 = interleukin-13 (see Figure 1 for other definitions).

Statistical analysis. GraphPad Prism was used for all statistical analyses. Group differences in serum ID-1 levels were evaluated by unpaired nonparametric Mann-Whitney U test or paired nonparametric Wilcoxon signed rank test. Correlations between serum ID-1 levels and clinical parameters were assessed by nonparametric Spearman's rank correlation. Results of cell proliferation assay and ELISAs used to detect cytokine expression were analyzed by unpaired parametric t-test. Levels of total citrullinated antigens in RA SF depleted of ID-1 were evaluated by paired nonparametric Wilcoxon signed rank test. Results are expressed as the mean ± SEM. Two-tailed P values less than 0.05 were considered significant.

RESULTS

Correlations between serum ID-1 levels and disease parameters, and effect of infliximab treatment. Serum ID-1 levels were measured in a Japanese cohort of 27 RA patients before and after infliximab treatment. We found that serum ID-1 levels were significantly elevated compared to those in age- and sex-matched normal controls (Figure 1A). Serum ID-1 levels before and 12 weeks after initiation of infliximab were compared. We observed a significant decrease in ID-1 levels after infliximab treatment (Figure 1B). Additionally, several clinical and laboratory parameters were measured, including matrix metallopeptidase 3 (MMP-3) level, erythrocyte sedimentation rate (ESR), the Disease Activity Score in 28 joints using ESR

(DAS28-ESR) (8), and the Simple Disease Activity Index (SDAI) (9), with significant improvements observed after infliximab treatment (Figure 1C). Next, baseline serum ID-1 levels were analyzed for correlation with disease parameters including RF, ESR, C-reactive protein (CRP) level, MMP-3 level, SDAI, Clinical Disease Activity Index (CDAI) (9), DAS28 using CRP level (DAS28-CRP), and DAS28-ESR. We found positive correlations between ID-1 levels and all of these parameters except RF (Figure 1D). Analysis using the change in SDAI score of responders and nonresponders after infliximab treatment showed that the serum ID-1 level correlated significantly with reduction in disease activity in the responders (24 of 27 patients) (Figure 1E).

In vitro targeting of ID-1 in RA FLS with the CRISPR/Cas9 system. We have previously shown that ID-1 is upregulated in RA synovium and that soluble ID-1 exhibits inflammatory and angiogenic properties (1,2). To examine the effects of ID-1 targeting in RA FLS by CRISPR/Cas9, cell proliferation assays were performed using the IncuCyte S3 Live Cell Analysis System. Results of ID-1 gene targeting were compared to those from the targeting of an irrelevant gene, *THBS1*. We achieved a maximum efficiency of 24.8% (Figure 2A), which was sufficient (due to an ample starting number of cells) for downstream experiments that used only the sorted RFP-positive cells. We found significant reductions in FLS growth beginning 13 hours after plating in culture (Figure 2B). To fully verify active and accurate genome editing by Cas9, transfected cells were sorted via FACS, and
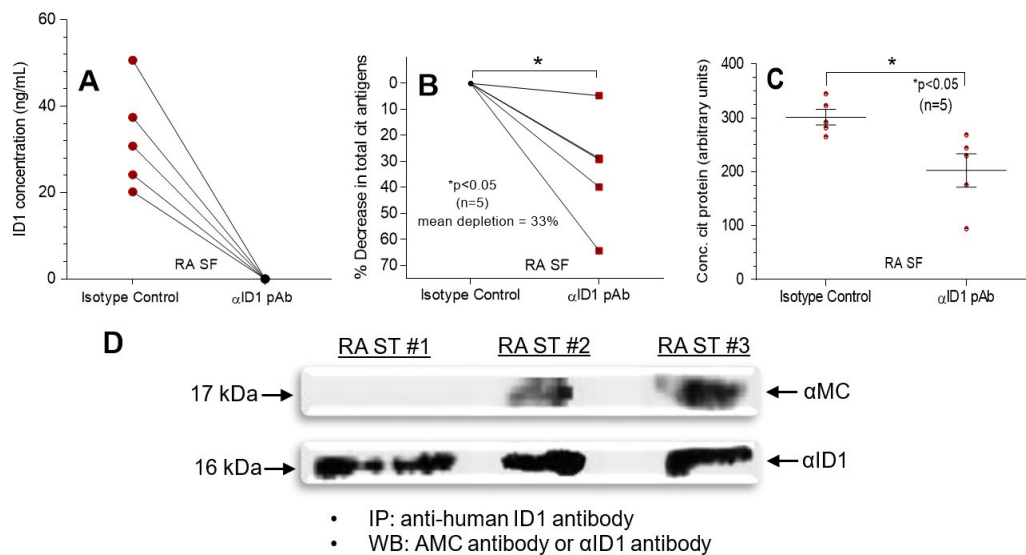

Figure 3. Immunodepletion of inhibitor of DNA binding 1 (ID-1) and detection of citrullinated ID-1 (cit–ID-1) in rheumatoid arthritis (RA) synovial fluid (SF) and synovial tissue (ST). **A**, Immunodepletion of ID-1 in RA SF (n = 5) using anti–ID-1 polyclonal antibody (pAb) was verified by enzyme-linked immunosorbent assay. **B**, Levels of total citrullinated antigens were measured in ID-1–depleted RA SF. Significant reduction in total citrullinated antigens after ID-1 depletion suggested that ID-1 is present in citrullinated forms in RA SF. **C**, Total citrullinated protein concentration in isotype control versus in anti–ID-1 antibody–treated RA SF was measured. Bars show the mean ± SEM. **D**, Detection of citrullinated forms of ID-1 in RA ST is shown. Immunoprecipitation (IP) was performed on RA ST homogenates using anti–ID-1 antibody, and blots were probed for ID-1 or total citrullinated antigens. Cit–ID-1 was detected in 2 of 3 RA ST homogenates. * = $P < 0.05$. WB = Western blotting; AMC = antimodified citrulline. Color figure can be viewed in the online issue, which is available at http://onlinelibrary.wiley.com/doi/10.1002/art.40886/abstract.

genomic DNA was isolated and sequenced. We then analyzed for aberrant sequences at the target site caused by indels of nonhomologous end–joining (NHEJ) using TIDE analysis (Figure 2C). We observed aberrant sequences and corresponding indel frequencies with an overall efficiency of 4.4% at the P value threshold of 0.001 with an R^2 of 0.99. To verify ID-1 depletion, Western blot analysis was performed on the sorted cells (Supplementary Figure 1, http://onlinelibrary.wiley.com/doi/10.1002/art.40886/abstract).

Decreased cellular proliferation and increased IL-6 and IL-8 production resulting from deletion of ID-1 in RA FLS. Sorted cells were cultured for 24 hours following overnight serum starvation, and supernatants were analyzed for cytokine expression (IL-13, ENA-78/CXCL5, IL-6, and IL-8) by ELISA (Figure 2D). RA FLS transfected with GFP control plasmid served as experimental control. We found significantly increased production of IL-6 and IL-8 compared to the controls, with no significant changes in IL-13 or ENA-78/CXCL5. RA FLS do not secrete appreciable amounts of IL-13, which was measured as a control cytokine in these experiments. RA FLS do spontaneously secrete ENA-78/CXCL5, as well as IL-6 and IL-8, but no substantial changes in ENA-78/CXCL5 levels were seen, indicating that the increases in IL-6 and IL-8 are specific effects of CRISPR/Cas9 targeting of the ID-1 gene.

Detection of cit–ID-1 in RA SF and ST. In the 2-step strategy to discover cit–ID-1, we first performed immunoprecipitation on RA SF using polyclonal antibodies independently to pull out both native and citrullinated forms of ID-1. Before proceeding to the second step, effective depletion of ID-1 from RA SF was verified using ELISA (Figure 3A). We then conducted an indirect ELISA on the depleted RA SF to detect total citrullinated antigens using antimodified citrulline (AMC) antibody (Supplementary Methods, http://onlinelibrary.wiley.com/doi/10.1002/art.40886/abstract). Depletion of ID-1 significantly reduced the level of the total citrullinated antigens in RA SF (Figure 3B). This suggests that the anti–ID-1 antibody that was used recognized both forms of ID-1, and that cit–ID-1 is present in RA SF. The data also showed that total citrullinated protein concentration was significantly higher in isotype controls versus anti–ID-1 antibody–treated SF samples (Figure 3C). Next, ID-1 immunoprecipitated from RA ST homogenates (using the same anti–ID-1 antibody) was analyzed by Western blotting using an AMC antibody (Supplementary Methods, http://onlinelibrary.wiley.com/doi/10.1002/art.40886/abstract). We detected a single prominent band (or complex of adjacent bands) when probing either for ID-1 directly with an anti–ID-1 antibody or for cit–ID-1 indirectly with an AMC antibody. Two of the 3 samples tested contained citrullinated forms of ID-1 (Figure 3D).

In vitro citrullination of rhID-1 protein. We incubated rhID-1 with rhPAD4 at various enzyme:substrate molar ratios in appropriate reaction buffer. To control for the potential confound-
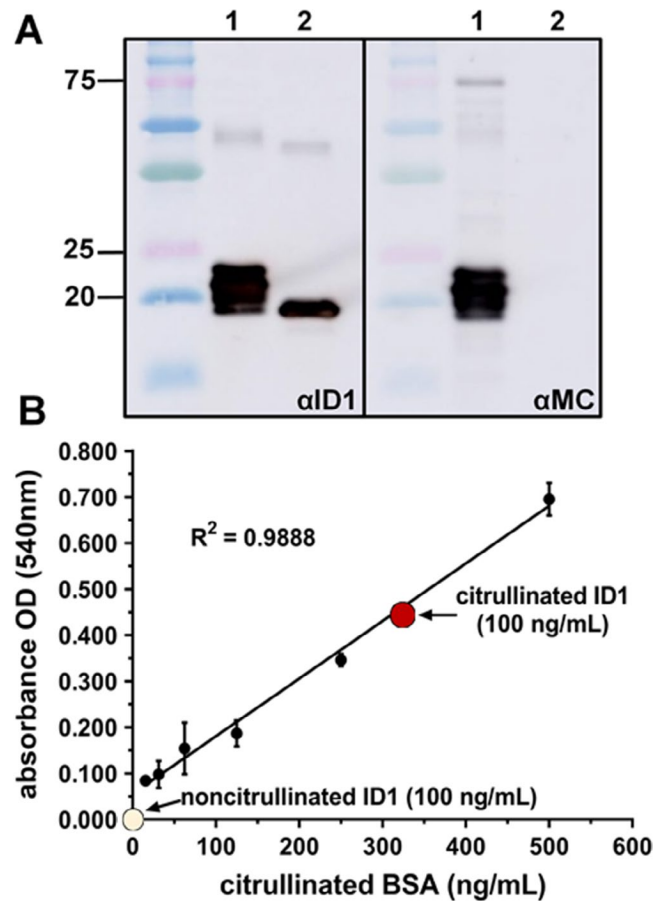

Figure 4. In vitro citrullination of recombinant human ID-1 (rhID-1) by recombinant human anti–peptidylarginine deiminase 4 (rhPAD4). **A**, Citrullination of rhID-1 by rhPAD4 was verified by Western blotting. Representative blots of cit–ID-1 (lane 1) and noncit–ID-1 (lane 2) were probed with anti–ID-1 or AMC antibodies. Cit–ID-1 exhibited multiple forms corresponding to the degree of modification and extended noticeably higher than noncit–ID-1, likely due to the increased hydrophobicity and the change in charge from the citrullination reaction. **B**, Citrullination of rhID-1 by rhPAD4 was verified via enzyme-linked immunosorbent assay (ELISA). Standard indirect ELISA protocol was modified to incorporate an acidic modification step for the AMC antibody as described. Cit–ID-1 and noncit–ID-1 can be distinguished by AMC antibody. Cit–ID-1 produced an OD equivalent to ~300 ng/ml of citrullinated bovine serum albumin (BSA), which was used as a relative standard due to its abundant modifiable arginines. Values are the mean ± SEM. See Figure 3 for other definitions. Color figure can be viewed in the online issue, which is available at http://onlinelibrary.wiley.com/doi/10.1002/art.40886/abstract.

ing effects of conditions and reaction buffer, parallel aliquots of rhID-1 were subjected to the same conditions except rhPAD4 was replaced with sterile water. To verify whether rhID-1 was citrullinated, we performed Western blotting and found that cit–ID-1 was recognized by the AMC antibody, while noncit–ID-1 was not recognized, as expected (Figure 4A). As a control, we also probed the samples using an anti–ID-1 antibody and confirmed that noncit–ID-1 was recognized (Figure 4A); cit–ID-1 was also recognized with this antibody, suggesting that citrullination did not alter its
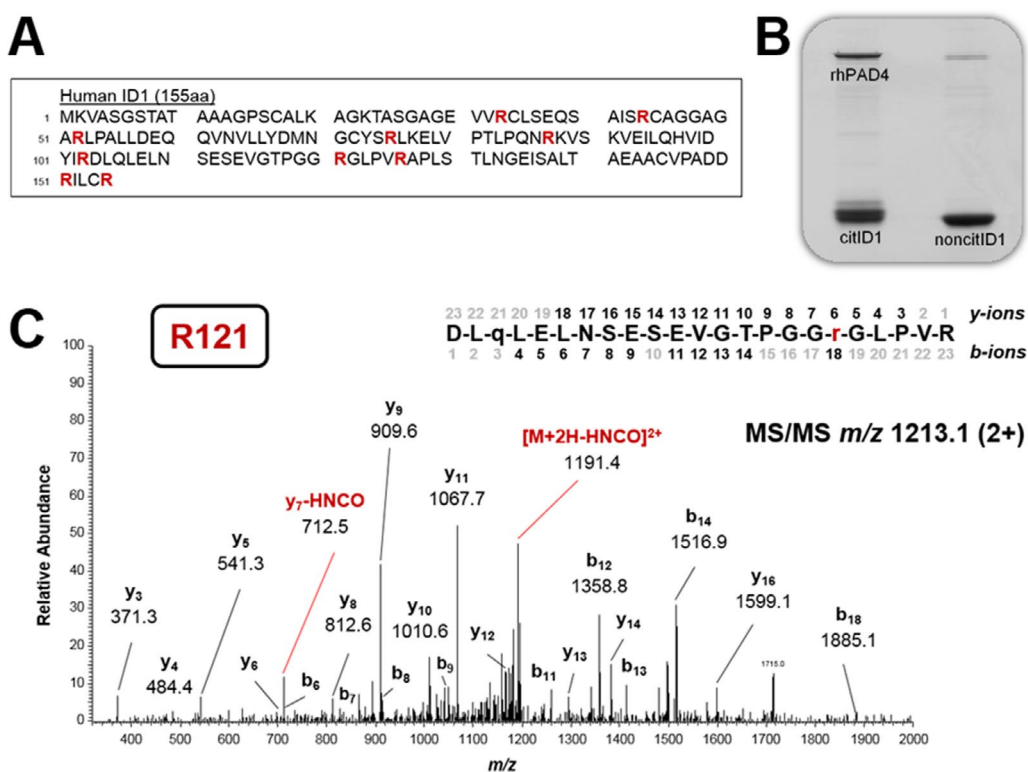
Figure 5. Liquid chromatography tandem mass spectrometry analysis (LC-MS/MS) of in vitro citrullinated recombinant human ID-1 (rhID-1). **A**, Sequence of human ID-1 isoform 1 is shown. Human ID-1 contains 10 arginines (R, highlighted red). RhID-1 was citrullinated in vitro by recombinant human anti–peptidylarginine deiminase 4 (rhPAD4) and analyzed via LC-MS/MS. **B**, Cit–ID-1 and noncit–ID-1 were run on sodium dodecyl sulfate–polyacrylamide gel electrophoresis and stained with "blue-silver" Coomassie for in-gel digestion prior to LC-MS/MS. **C**, The annotated mass spectrum of tryptic peptide confirmed citrullination of R121 in rhID-1. All detected ions of the peptide are shown in black in the sequence and are annotated in the spectrum. The red r denotes citrulline. Ions highlighted in red in the spectrum show the neutral loss of isocyanic acid (HNCO; ~43 daltons), diagnostic marker ions for citrullination. See Figure 3 for other definitions. Color figure can be viewed in the online issue, which is available at http://onlinelibrary.wiley.com/doi/10.1002/art.40886/abstract.

epitope and that both forms can be recognized by a single antibody. In addition, we performed ELISAs using the AMC antibody on cit–ID-1 for further confirmation of citrullination. We observed a markedly higher absorbance in the cit–ID-1 sample as compared to that of the noncit–ID-1 sample (Figure 4B). Citrullinated BSA (cit-BSA) was used as a positive control for citrullination and as a relative standard for this ELISA.

LC-MS/MS identification of specific citrullines in in vitro–citrullinated rhID-1. Human ID-1 contains 10 arginines (Figure 5A), all of which are potential candidates for citrullination by PAD enzymes. We found that cit–ID-1 extends visibly higher than noncit–ID-1 on a gel (Figure 5B), likely due to the increase in hydrophobicity and the change in charge from positive to neutral due to the citrullination reaction. Subsequently, the samples were analyzed by LC-MS/MS to detect the site(s) of citrullination based on the tandem MS fragmentation pattern and the expected neutral loss of isocyanic acid that is diagnostic for citrullination in MS (10). We found multiple citrullinated arginines, varying in number depending on the batch of rhID-1 and the experimental conditions of in vitro citrullination. Arginine R121 was consistently citrullinated by rhPAD4,

as shown in a representative spectrum (Figure 5C). Interestingly, LC-MS/MS analysis identified native citrulline residues in the noncit–ID-1 samples, which were expected from the production of rhID-1 in HEK 293T cells. However, with Western blot analysis using an AMC antibody these citrulline residues were not recognized (Figure 4A), suggesting that LC-MS/MS analysis is a more sensitive technique to identify low-level constitutive citrullination.

Measurement of ACPA reactivity with cit–ID-1 in normal and RA PB sera and RA SF. We found positive ACPA reactivity against cit–ID-1 but not against noncit–ID-1, in RA PB sera and SF (Figure 6A). All antigens, including control antigens (noncit–ID-1, BSA, cit-BSA, ENA-78, citENA-78, as well as rhPAD4 [data not shown]), were dotted in triplicate on the same blot and probed together in the same patient sample to ensure citrulline-specific binding by the ACPAs. All control blots showed no significant evidence of antibody binding but did show positivity for cit–ID-1 (Supplementary Figure 2, http://onlinelibrary. wiley.com/doi/10.1002/art.40886/abstract). Normal sera were used as controls, and no reactivity was observed. To control for nonspecific serum antibody binding, human IgG was used at a
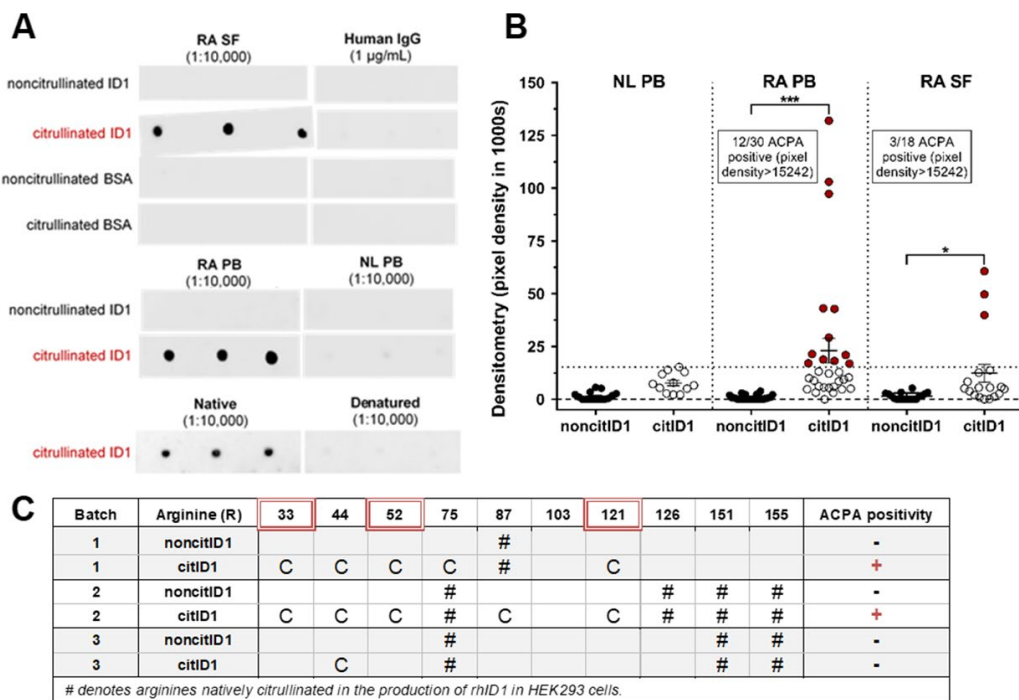
Figure 6. Detection of anti–citrullinated protein antibodies (ACPAs) to cit–ID-1 RA samples. **A**, RA SF, RA sera, and normal (NL) sera were assayed for autoantibodies to cit–ID-1 by immunodot blotting. ACPA reactivity with cit–ID-1, but not native ID-1, was found in RA SF and peripheral blood (PB), but not in normal PB. Human IgG (1 μg/ml) was used as a control and showed no reactivity. Additionally, ACPAs from RA PB did not bind when cit–ID-1 was boiled (denatured). Control dots showed no significant evidence of ACPAs or antibody binding reactivity in RA SF, RA PB, or normal PB. **B**, Analysis of immunodot blots via densitometry showed higher reactivity with cit–ID-1 than noncit–ID-1 in RA PB (n = 30 samples from 10 patients) and in RA SF (n = 18 samples from 6 patients), but not in normal PB (n = 12 samples from 4 patients). Bars show the mean ± SEM. Dotted line represents the cutoff value used to determine positive reactivity (red dots) in experimental samples. Values were derived from the highest white point in healthy control samples. * = P < 0.05; *** = P < 0.001. **C**, Analysis of the roles of individual citrulline residues in ACPA reactivity of in vitro citrullinated rhID-1 is shown. Arginines R33, R52, and R121 were critically necessary for ACPA reactivity. C denotes citrullines; # denotes native citrullines from the production of rhID-1 in HEK 293 cells. BSA = bovine serum albumin (see Figure 3 for other definitions). Color figure can be viewed in the online issue, which is available at http://onlinelibrary.wiley.com/doi/10.1002/art.40886/abstract.

relatively high dilution (1 μg/ml). Furthermore, all additional control antibodies were negative (data not shown). By densitometry analysis of immunodot blotting, we found that 40% of RA sera recognized cit–ID-1 versus no control sera. SF from 16.7% of RA patients tested positive for anti–cit–ID-1 (Figure 6B).

Identification of the critical arginines conferring autoantigenicity to cit–ID-1. Immunodot blot analysis for ACPA reactivity showed that cit–ID-1 displayed unique autoantigenicity and autoantibody reactivity, depending on the citrullination pattern. Specifically, samples that showed reactivity with batches 1 and 2 did not shown any reactivity with batch 3, likely due to the lack of key epitopes. Thus, a batch was designated ACPA positive if it showed reactivity with any of the limited patient samples. We did not observe any ACPA binding to the baseline-modified arginines that were present in rhID-1 obtained from the vendor. Using a series of LC-MS/MS and immunodot blot analyses, we identified key arginines in rhID-1 that may be autoantigenic targets for ACPA development in RA. Of the 10 available arginines in rhID-1, the critical arginines for ACPA reactivity were located at positions R33, R52, and R121 (Figure 6C).

To further study the role of these arginines, citrullinated peptides (12 amino acids in length) spanning these regions were tested but were negative for ACPA binding (data not shown). Moreover, denaturing of cit–ID-1 before immunodot blotting negated its reactivity (Figure 6A). Thus, the critical arginines at R33, R52, and R121 may control conformational epitopes that render cit–ID-1 antigenic in vivo. These data corroborate our observation that multiple forms of ID-1 are expressed in vitro and in vivo, but only certain modified forms bind ACPAs (Figure 4A).

DISCUSSION

As a nuclear protein that alters the activity of many transcription factors, ID-1 appears to affect multiple cellular properties including proinflammatory cytokine expression. This would place ID-1 in a strategic position to regulate chronic inflammatory responses directly by inhibition of cytokine production at the transcriptional level. Such regulatory activity could profoundly influence the severity and progression of inflammatory outcomes in chronic diseases including RA. There is mounting evidence that permanently altered FLS function is the result of somatic mutations in key genes that

regulate the FLS cell cycle, proliferation, and apoptosis (11,12). It has also been suggested that RA synoviocytes have characteristics similar to those of tumor cells, as a number of oncogenes involved in cell cycle regulation—or those that act as transcription factors, such as c-*Fos*, *c-ras*, *c-raf*, *c-myc*, and *c-myb*—are expressed at high levels in RA FLS (12). We explored the possibility that another nuclear regulatory protein, namely ID-1, plays a central role in RA pathogenesis, independent of tumor necrosis factor, both by regulating cytokine secretion and as an inflammatory protein that can undergo posttranslational modifications.

We successfully transfected primary RA FLS with a plasmid containing a CRISPR/Cas9 construct, demonstrated successful ID-1 gene targeting using a TIDE algorithm and output analysis (6), and confirmed these findings by FACS and Western blot analysis. We found substantial increases in IL-6 (30-fold) and IL-8 (50-fold) but not in ENA-78/CXCL5 in supernatants from transfected FLS, compared to sham-transfected control FLS. Using a cell imaging system, we also found that FLS deleted of ID-1 showed a >20% sustained reduction in proliferation. This may be due in part to elevated production of IL-6, a cytokine known to inhibit fibroblast proliferation (13). More likely, a permanent mutation in an important nuclear regulatory protein that is critical for cell proliferation may have altered the FLS population into a phenotype capable of elevated proinflammatory cytokine secretion. Notably, it has been shown that ID-1 antisense RNA prevents early-passage fibroblasts from entering the S phase of the cell cycle (14). Firestein et al proposed a model suggesting a duality of FLS populations labeled "passive responders" and "transformed aggressors" (12), which arose partly from the combination of a highly inflamed environment in the RA joint and somatic mutations. Thus, both the data from the current study and previously reported findings suggest that FLS proliferation and heightened FLS secretion of IL-6 represent distinct stages of the contributions of FLS to the pathogenesis of RA. Moreover, the current findings indicate that ID-1 can mediate transition of FLS between these two important pathogenic phases.

Analysis of clinical specimens revealed that soluble ID-1 is present and up-regulated in the serum of RA patients and shows a significant positive correlation with a number of disease parameters including ESR, CRP level, MMP-3 level, SDAI, CDAI, DAS28-CRP, and DAS28-ESR. This indicates that circulating serum ID-1 levels could be a potential biomarker for RA severity. Additionally, because serum ID-1 concentration does not correlate with RF titer, it is possible to identify patients with RF-negative RA whose disease will be severe, by measurement of elevated ID-1. Furthermore, after 12 weeks of infliximab, serum levels of ID-1 showed significant reductions. We found that 24 of 27 patients responded to infliximab (based on the SDAI) and that reduction in the level of ID-1 significantly correlated with reduction in disease activity in the responders. Because of the elevated circulating concentrations of ID-1, we surmised that citrullinated forms of ID-1 could be present and immunogenic in RA patients, as autoantibodies to citrul-

linated proteins are well-known disease-associated phenomena in RA (15–19).

ACPAs are implicated in RA pathogenesis in synergy with smoking, an environmental risk factor for RA, and the shared epitope major histocompatibility complex allele (20). However, the full range of citrullinated autoantigens in RA is not yet defined. We showed that ID-1 can be citrullinated in vitro. Moreover, by depleting ID-1 from RA SFs we reduced the total amount of citrullinated proteins detected by as much as 64% (mean 33%) as measured by cit-ELISA. We also found, by immunoblotting, that a subset of RA patients had high-titer autoantibodies to cit–ID-1. Therefore, cit–ID-1 in RA SF may account for a significant portion of citrullinated proteins that are the targets of the ACPA response in some RA patients.

Next, we performed immunodot blotting with RA and normal PB sera, as well as RA SF, against various citrullinated and noncitrullinated proteins. We were able to confirm the presence of ACPAs to cit–ID-1 in both RA sera and SF but not in the PB from healthy individuals, which supports our hypothesis that citrullination of ID-1 increases its autoantigenicity in RA. Experiments using immunodot blotting for ID-1 and cit–ID-1 revealed that antibodies to cit–ID-1 can be detected in RA sera and SF. In SF, the presence of large amounts of cit–ID-1 could sequester anti–cit–ID-1 in immune complexes, which could then incorporate RF and therefore be undetectable by the cit-ELISAs. Such mechanisms could account for the relatively low frequency of positivity for anti–cit–ID-1 in SF samples.

Various citrullinated forms of ID-1 may function differently as agonists or autoantigens, complicating the analysis of cit–ID-1 activity. This is because citrullination reactions with the PAD enzyme are notoriously inconsistent, resulting in differences in the number and patterns of arginines that are converted to citrullines. These inconsistencies make it difficult to determine the extent to which citrullination of ID-1 leads to alterations in its activity. Indeed, we have found that the number and locations of arginines citrullinated in ID-1 can change by simply altering the source of the PAD enzyme used in the reaction mix. Moreover, many of the mechanistic roles of ACPAs remain unknown. Notably, Schett et al reported that autoantibody to citrullinated vimentin directly induces bone loss, providing a mechanism for osteopenia in early or preclinical RA (21,22). In the case of the chemokine IL-8/CXCL8, only 1 of 3 arginines was citrullinated, yet this resulted in alteration of function (23). Another example in which citrullination of a single arginine by these methods resulted in functional changes occurred in stromal cell–derived factor 1 CXCL12 (24).

We found that some forms of cit–ID-1 can be highly reactive with ACPAs formed in RA but that less deiminated forms do not retain autoantigenicity. It appears that the degree of citrullination of ID-1 may alter the folding pattern and immune properties of ID-1, leading to autoantigenicity. We have previously investigated the autoantigenicity of citrullinated ENA-78/CXCL5, which is also highly up-regulated in RA (7). Similar to cit–ID-1,

citrullination of ENA-78/CXCL5 at arginine R48 enabled binding to ACPA in RA sera and SF in our assays. Furthermore, we previously showed that citrullination of ENA-78/CXCL5 induced a functional change in the protein from a neutrophil chemoattractant to a monocyte chemoattractant (7). Since citrullination of a protein with only 2 arginines, such as ENA-78/CXCL5, can cause a profound increase in autoantigenicity and change in function, the impact citrullination can have on ID-1, which contains 10 arginines, could be very substantial.

Through detailed LC-MS/MS analysis, we observed conversions of ID-1 in all but 1 arginine at R103, perhaps explained by structural unavailability or PAD preference for certain arginines. As an example, the annotated fragmentation spectrum presented in Figure 5 shows the ions corresponding to the partial sequence of ID-1 around arginine 121. These ions show the neutral loss of isocyanic acid resulting from the fragmentation of the ureido group in citrullines, which is a marker for citrullination, confirming the modification of ID-1. Through a series of citrullination reactions followed by LC-MS/MS, we identified that the modifications at arginines R33, R52, and R121 in cit–ID-1 can bind to and perhaps induce ACPAs. However, small peptides spanning these regions were not reactive with RA serum, and boiling cit–ID-1 before immunodot blot assays negated binding by RA sera. Overall, the data is most consistent with a model that involves recognition by ACPA of conformational, but not linear, autoantigen epitopes on cit–ID-1.

We previously reported that ID-1 is secreted by inflammatory FLS and is an angiogenic mediator (1,2). It is possible that free ID-1 is citrullinated either in FLS and/or extracellularly in the inflamed RA joint to render it autoantigenic in RA tissues. We demonstrated a potential role of ID-1 in transforming FLS into a pathogenic phenotype and identified cit–ID-1 as a novel autoantigen candidate in RA. Further investigation is needed to determine whether and how citrullination of ID-1 may alter its functions. Potentially, ID-1, cit–ID-1, and/or ACPAs to cit–ID-1 may serve as promising therapeutic targets or biomarkers in RA.

ACKNOWLEDGMENTS

AUTHOR CONTRIBUTIONS

All authors were involved in drafting the article or revising it critically for important intellectual content, and all authors approved the final version to be published. Mr. Ohara had full access to all of the data in the study and takes responsibility for the integrity of the data and the accuracy of the data analysis.

Study conception and design. Ohara, Edhayan, Rasmussen, Isozaki, Remmer, Lanigan, Campbell, Fox, Ruth.

Acquisition of data. Ohara, Edhayan, Rasmussen, Isozaki, Urquhart, Lawton, Chung, Fox.

Analysis and interpretation of data. Ohara, Edhayan, Rasmussen, Isozaki, Remmer, Lanigan, Campbell, Fox, Ruth.

REFERENCES

1. Isozaki T, Amin MA, Arbab AS, Koch AE, Ha CM, Edhayan G, et al. Inhibitor of DNA binding 1 as a secreted angiogenic transcription factor in rheumatoid arthritis. Arthritis Res Ther 2014;16:R68.

2. Edhayan G, Ohara RA, Stinson WA, Amin MA, Isozaki T, Ha CM, et al. Inflammatory properties of inhibitor of DNA binding 1 secreted by synovial fibroblasts in rheumatoid arthritis. Arthritis Res Ther 2016;18:87.

3. Mor-Vaknin N, Punturieri A, Sitwala K, Faulkner N, Legendre M, Khodadoust MS, et al. The DEK nuclear autoantigen is a secreted chemotactic factor. Mol Cell Biol 2006;26:9484–96.

4. Mor-Vaknin N, Kappes F, Dick AE, Legendre M, Damoc C, Teitz-Tennenbaum S, et al. DEK in the synovium of patients with juvenile idiopathic arthritis: characterization of DEK antibodies and posttranslational modification of the DEK autoantigen. Arthritis Rheum 2011;63:556–67.

5. Arnett FC, Edworthy SM, Bloch DA, McShane DJ, Fries JF, Cooper NS, et al. The American Rheumatism Association 1987 revised criteria for the classification of rheumatoid arthritis. Arthritis Rheum 1988;31:315–24.

6. Brinkman EK, Chen T, Amendola M, van Steensel B. Easy quantitative assessment of genome editing by sequence trace decomposition. Nucleic Acids Res 2014;42:e168.

7. Yoshida K, Korchynskyi O, Tak PP, Isozaki T, Ruth JH, Campbell PL, et al. Citrullination of epithelial neutrophil–activating peptide 78/CXCL5 results in conversion from a non–monocyte-recruiting chemokine to a monocyte-recruiting chemokine. Arthritis Rheumatol 2014;66:2716–27.

8. Prevoo ML, van 't Hof MA, Kuper HH, van Leeuwen MA, van de Putte LB, van Riel PL. Modified disease activity scores that include twenty-eight–joint counts: development and validation in a prospective longitudinal study of patients with rheumatoid arthritis. Arthritis Rheum 1995;38:44–8.

9. Aletaha D, Smolen J. The Simplified Disease Activity Index (SDAI) and the Clinical Disease Activity Index (CDAI): a review of their usefulness and validity in rheumatoid arthritis. Clin Exp Rheumatol 2005;23 Suppl 39:S100–8.

10. Hao G, Wang D, Gu J, Shen Q, Gross SS, Wang Y. Neutral loss of isocyanic acid in peptide CID spectra: a novel diagnostic marker for mass spectrometric identification of protein citrullination. J Am Soc Mass Spectrom 2009;20:723–7.

11. Han Z, Boyle DL, Shi Y, Green DR, Firestein GS. Dominant-negative p53 mutations in rheumatoid arthritis. Arthritis Rheum 1999;42:1088–92.

12. Bartok B, Firestein GS. Fibroblast-like synoviocytes: key effector cells in rheumatoid arthritis. Immunol Rev 2010;233:233–55.

13. Nishimoto N, Ito A, Ono M, Tagoh H, Matsumoto T, Tomita T, et al. IL-6 inhibits the proliferation of fibroblastic synovial cells from rheumatoid arthritis patients in the presence of soluble IL-6 receptor. Int Immunol 2000;12:187–93.

14. Hara E, Yamaguchi T, Nojima H, Ide T, Campisi J, Okayama H, et al. Id-related genes encoding helix-loop-helix proteins are required for G1 progression and are repressed in senescent human fibroblasts. J Biol Chem 1994;269:2139–45.

15. Clavel C, Nogueira L, Laurent L, Iobagiu C, Vincent C, Sebbag M, et al. Induction of macrophage secretion of tumor necrosis factor α through Fcγ receptor IIa engagement by rheumatoid arthritis-specific autoantibodies to citrullinated proteins complexed with fibrinogen. Arthritis Rheum 2008;58:678–88.

16. Sokolove J, Zhao X, Chandra PE, Robinson WH. Immune complexes containing citrullinated fibrinogen costimulate macrophages via Toll-like receptor 4 and Fcgγ receptor. Arthritis Rheum 2011;63:53–62.

17. Pratesi F, Dioni I, Tommasi C, Alcaro MC, Paolini I, Barbetti F, et al. Antibodies from patients with rheumatoid arthritis target citrullinated histone 4 contained in neutrophils extracellular traps. Ann Rheum Dis 2014;73:1414–22.

18. Wigerblad G, Bas DB, Fernades-Cerqueira C, Krishnamurthy A, Nandakumar KS, Rogoz K, et al. Autoantibodies to citrullinated proteins induce joint pain independent of inflammation via a chemokine-dependent mechanism. Ann Rheum Dis 2016;75:730–8.

19. Habets KL, Trouw LA, Levarht EW, Korporaal SJ, Habets PA, de Groot P, et al. Anti-citrullinated protein antibodies contribute to platelet activation in rheumatoid arthritis. Arthritis Res Ther 2015;17:209.

20. Klareskog L, Stolt P, Lundberg K, Källberg H, Bengtsson C, Grunewald J, et al. A new model for an etiology of rheumatoid arthritis: smoking may trigger HLA–DR (shared epitope)–restricted immune reactions to autoantigens modified by citrullination. Arthritis Rheum 2006;54:38–46.

21. Harre U, Georgess D, Bang H, Bozec A, Axmann R, Ossipova E, et al. Induction of osteoclastogenesis and bone loss by human autoantibodies against citrullinated vimentin. J Clin Invest 2012;122:1791–802.

22. Engdahl C, Bang H, Dietel K, Lang SC, Harre U, Schett G. Periarticular bone loss in arthritis is induced by autoantibodies against citrullinated vimentin. J Bone Miner Res 2017;32:1681–91.

23. Proost P, Loos T, Mortier A, Schutyser E, Gouwy M, Noppen S, et al. Citrullination of CXCL8 by peptidylarginine deiminase alters receptor usage, prevents proteolysis, and dampens tissue inflammation. J Exp Med 2008;205:2085–97.

24. Struyf S, Noppen S, Loos T, Mortier A, Gouwy M, Verbeke H, et al. Citrullination of CXCL12 differentially reduces CXCR4 and CXCR7 binding with loss of inflammatory and anti-HIV-1 activity via CXCR4. J Immunol 2009;182:666–74.